Functional Interactions in Cytochrome $P450_{BM3}$. Evidence That NADP(H) Binding Controls Redox Potentials of the Flavin Cofactors†

Marat B. Murataliev* and René Feyereisen

Department of Entomology and Center for Toxicology, University of Arizona, Tucson, Arizona 85721

Received May 10, 2000; Revised Manuscript Received August 2, 2000

ABSTRACT: NADP(H) binding is essential for fast electron transfer through the flavoprotein domain of the fusion protein P450BM3. Here we characterize the interaction of NADP(H) with the oxidized and partially reduced enzyme and the effect of this interaction on the redox properties of flavin cofactors and electron transfer. Measurements by three different approaches demonstrated a relatively low affinity of oxidized P450BM3 for $NADP^+$, with a K_d of about 10 μM. NADPH binding is also relatively weak (K_d ~10 μM), but the affinity increases manyfold upon hydride ion transfer so that the active 2-electron reduced enzyme binds $NADP^+$ with a K_d in the submicromolar range. NADP(H) binding induces conformational changes of the protein as demonstrated by tryptophan fluorescence quenching. Fluorescence quenching indicated preferential binding of NADPH by oxidized P450BM3, while no catalytically competent binding with reduced P450BM3 could be detected. The hydride ion transfer step, as well as the interflavin electron transfer steps, is readily reversible, as demonstrated by a hydride ion exchange (transhydrogenase) reaction between NADPH and $NADP^+$ or their analogues. Experiments with FMN-free mutants demonstrated that FAD is the only flavin cofactor required for the transhydrogenase activity. The equilibrium constants of each electron transfer step of the flavoprotein domain during catalytic turnover have been calculated. The values obtained differ from those calculated from equilibrium redox potentials by as much as 2 orders of magnitude. The differences result from the enzyme's interaction with NADP(H).

The flavoprotein domain of cytochrome $P450_{BM3}$ belongs to a family of homologous flavoenzymes utilizing both FAD and FMN cofactors to transfer reducing equivalents from NADPH to hemoproteins or other electron acceptors (*1*). Cytochrome P450 reductase and the flavoprotein subunit of sulfite reductase are individual polypeptides. The flavoprotein domains of fatty acid hydroxylating cytochromes $P450_{BM3}$ (*2*−*4*) and P450foxy (*5*), as well as of nitric oxide synthase (for reviews, see refs *6* and *7*), are fused in a single polypeptide with the hemoprotein domains.

The two flavin cofactors have different roles in catalysis: FAD accepts a hydride ion from NADPH and passes electrons to the FMN, which in turn delivers electrons to the P450 or other acceptors (*8*−*10*). The equilibrium redox potentials determined for the P450BM3[1] flavoprotein domain (*11*) are inconsistent with our current understanding of the catalytic mechanism. According to these values, a catalytically inactive FMN hydroquinone form should be formed in milliseconds after enzyme reduction by NADPH. In contrast, most of the 2-electron reduced enzyme is present as a double semiquinone form, and the inactivation rate is almost 4 orders of magnitude slower than the rates of electron transfer (*12*).

Another aspect of catalysis which remains unclear is the role of nucleotide in electron transfer. A comparison of the catalytic rates of P450BM3 and P450 reductase showed that NADP(H) binding is essential for fast transfer of reducing equivalents through the flavins and that NADP(H) interaction with the flavoprotein can control the redox properties of the flavin cofactors (*12*−*14*). The important role of NADP(H) binding in the catalytic mechanism of P450BM3 warrants a more thorough characterization of its interactions with nucleotides. However, only limited studies have addressed the interaction of P450BM3 with NADP(H) (*15*).

Previously, we characterized the nucleotide specificity of P450BM3 and measured the K_m values for fatty acid hydroxylase and cytochrome *c* reductase activities (*12*). In this paper, we present our studies of P450BM3 interaction with NADP(H) and their analogues. The affinities for both oxidized and reduced nucleotides have been determined, and the transhydrogenase activities of the wild type, as well as mutant P450BM3, have been characterized. The results allowed us to estimate the dynamic distribution of the catalytic intermediates of the flavoprotein domain during catalysis, which is quite different from that expected from the equilibrium redox potentials of the flavin cofactors.

† This work was supported by National Institutes of Health Grants GM39014 and ES06694.

* To whom correspondence should be addressed: Department of Entomology, Forbes 410, P.O. Box 210036, University of Arizona, Tucson, AZ 85721-0036. Tel: (520)-621-9547. Fax: (520)-621-1150. E-mail: marat@ag.arizona.edu.

[1] Abbreviations: AcPy-NADP(H), 3-acetylpyridine−NADP(H); BMR, flavoprotein domain of the P450BM3; G6P-DH, glucose-6-phosphate dehydrogenase; H_4-NADP, 1,4,5,6-tetrahydro-NADP; P450PM3, cytochrome $P450_{BM3}$ isolated from *Bacillus megaterium*; P450 reductase, NADPH−cytochrome P450 reductase; S-NADP(H), thionicotinamide−NADP(H); TLC, thin-layer chromatography.

10.1021/bi001068u CCC: $19.00
Published on Web 09/20/2000

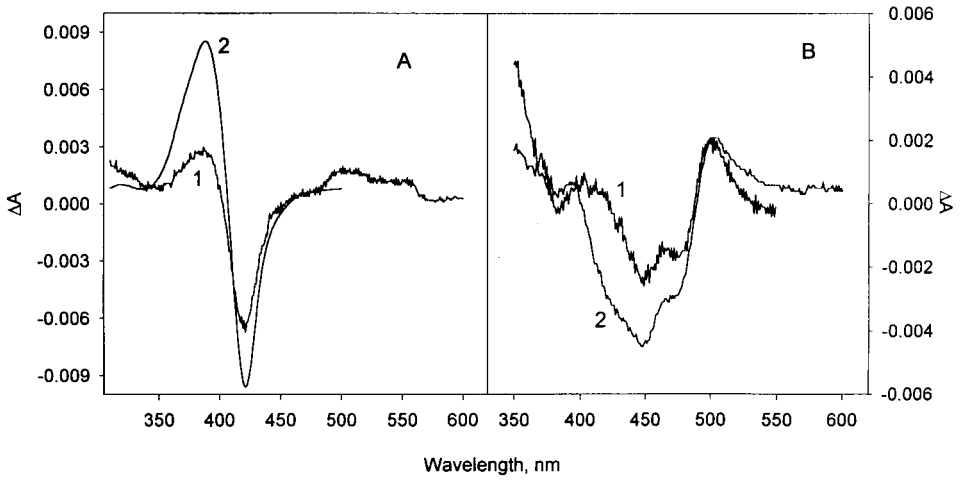

FIGURE 1: (A) Spectral changes associated with $NADP^+$ and palmitate binding with intact P450BM3. The $NADP^+$-induced difference spectrum (spectrum 1) was recorded with 0.6 μM P450BM3 and 7.5 μM $NADP^+$. The type I spectrum (spectrum 2) was recorded in the presence of 2.3 μM P450BM3 and 25 μM palmitate. The amplitude of this spectrum was reduced 16 times for easier comparison. (B) Spectral changes induced by $NADP^+$ with palmitate-saturated P450BM3 (spectrum 1) and BMR (spectrum 2). Concentrations were as follows: P450BM3, 6.0 μM, palmitate, 75 μM, and $NADP^+$, 50 μM, for spectrum 1 and BMR, 9.2 μM, and $NADP^+$, 10 μM, in spectrum 2.

MATERIALS AND METHODS

Preparative Procedures. Wild type and mutant P450BM3 as well as BMR were purified as described earlier (*16*). Preparation of [^{32}P]NADP was carried out as described before (*17*). [^{3}H]$NADP^+$ was synthesized by the same procedure. The specific activity of [^{32}P]NADP(H) was 660 cpm/pmol, while that of [^{3}H]nucleotide was 1 μCi/nmol. 1,4,5,6-Tetrahydro-NADP was prepared as described (*14*).

Measurements of the Tryptophan Fluorescence Spectra. Tryptophan fluorescence emission spectra were measured on a Photon Technology Instrument spectrofluorometer in a final volume of 2.5 mL at 25 °C at λ_{ex} 295 nm and λ_{em} 310−500 nm. The excitation light of 295 nm was chosen to minimize the contribution of Tyr residues. The time course of Trp fluorescence change was recorded at λ_{ex} 295 nm and λ_{em} 334 nm.

Activity Assay. All the assays were carried out at 25 °C in 0.1 M Tris-HCl buffer, pH 7.7, as detailed earlier (*12*). Transhydrogenase activities with AcPy-NADP(H) and S-NADP(H) were measured spectrophotometrically, and NADPH−[^{3}H]$NADP^+$ activity was measured using HPLC separation of the nucleotides as described for P450 reductase (*14*).

Fluorometric measurement of palmitate-dependent NADPH oxidation was carried out as follows. The reaction mixture (2.5 mL) contained 25 μM palmitate and 0.4−5.0 μM NADPH. The reaction was started by the addition of P450BM3 to a final concentration of 1−6 nM, and the reaction was monitored by fluorescence decrease at 455 nm with λ_{ex} = 340 nm. Data were collected at a rate of 10/s. The initial reaction rates were calculated from the fluorescence decrease slopes in the first 5−6 s of the reaction after scale calibration with a standard NADPH solution. Fluorescence intensity was proportional to NADPH concentration up to 5 μM. In inhibition studies 0−40 μM $NADP^+$ was included in the assay.

Interaction of P450BM3 with Nucleotides. Binding of ^{32}P-radiolabeled nucleotides was carried out using a microfiltration procedure as described elsewhere (*14*). [^{32}P]-nucleotide composition was measured as described earlier (*17*). Briefly, [^{32}P]NADPH was incubated with P450BM3, and at the time indicated, aliquots were quenched with equal volume of 2% SDS solution and nucleotides were quantified after separation by TLC on poly(ethylenimine)−cellulose plates.

Spectroscopic studies of nucleotide binding were carried out in a 1 mL reaction mixture at 25 °C. Protein concentrations are indicated in the legends to the figures. Nucleotide solution was added to both sample and reference cuvettes. The total volume added did not exceed 2% of the reaction mixture, and no correction was made.

Other Procedures. Protein concentration was determined by the Lowry procedure (*18*) using bovine serum albumin as a standard. The values presented are the mean ± SD of at least three measurements. The molar concentration of P450BM3 was calculated on the basis of the protein content using a molecular mass of 119 000 Da (*2*).

RESULTS AND DISCUSSION

Spectroscopic Studies of $NADP^+$ Interaction with P450BM3. The interaction of P450BM3 with nucleotides has not been studied in detail. It was reported (*15*) that P450BM3 binds $NADP^+$ with a K_d of 0.58 μM. The measurements were based on the spectral changes of P450BM3 induced by $NADP^+$, and $\Delta A_{421-475}$ was plotted as a function of the nucleotide concentration. We repeated these experiments. Addition of $NADP^+$ to the P450BM3 solution resulted in a slight perturbation of the absorption spectrum of P450BM3. The difference spectrum showed a decrease in absorbance at 421 nm and little change at 475 nm (Figure 1A, spectrum 1). The dependence of the absorbance change on $NADP^+$ concentration gave a K_d value of about 0.7 μM (not shown), in good agreement with the previous report (*15*).

However, when the $NADP^+$ absorbance difference spectrum was compared to that induced by palmitate binding (Figure 1A, spectrum 2), we found that the spectral changes were remarkably similar. Palmitate shifted the heme absorbance maximum from 420 to 390 nm, which reflects the

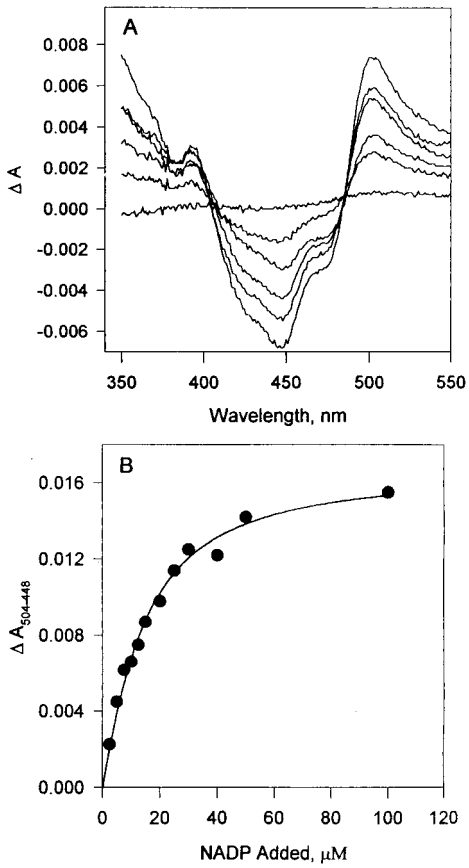

FIGURE 2: Spectral changes associated with $NADP^+$ binding with BMR. (A) Difference spectra obtained in the presence of 5, 10 20, 30, and 50 μM $NADP^+$. (B) Dependence of the amplitude of spectral changes on $NADP^+$ concentration. The BMR concentration was 9.2 μM, 1 mL final volume, and 2.5 or 5 mM $NADP^+$ solutions were added. The reference cell contained BMR, and buffer was added instead of $NADP^+$. The total volume added did not exceed 2%. The best fit of the experimental points to eq 1 gave a K_d of 9.4 μM and an A_{max} of 1.84 AU/mM. The line represents the binding curve calculated according to eq 1 using these parameters.

transition of low spin to high spin of the heme iron (type I binding spectrum). Thus in $NADP^+$ binding experiments with intact P450BM3, the trough at 421 nm could correspond to the decreased heme absorption. To verify this, P450BM3 was converted to a high-spin form by the addition of saturating palmitate, $NADP^+$ was added, and the difference spectrum was recorded (Figure 1B, spectrum 1). Small spectral changes at 400−550 nm were observed. These spectral changes were similar to those induced by the nucleotide in the separately expressed flavoprotein domain, BMR (spectrum 2). These results indicate that heme spectral changes interfered with the spectrophotometric measurements of nucleotide binding to intact P450BM3.

Spectroscopic Studies of $NADP^+$ Interaction with BMR. To exclude any interference of the heme, the binding experiments were carried out with BMR. Addition of $NADP^+$ to the BMR solution induced small spectral changes (Figure 2A). The absorbance at 448 nm decreased while the absorbance at 504 nm increased upon addition of $NADP^+$. Neither NAD^+ nor 2′-AMP at 100 μM induced spectral changes in BMR (data not shown). The amplitude of the spectral perturbation depended on the $NADP^+$ concentration and was used for estimation of the K_d. Because of the relatively small spectral changes, a BMR concentration of 9.2 μM was used. Under these conditions, a considerable fraction of the added $NADP^+$ was bound, and a binding curve was calculated using a mutually depleting model (*19*). The amplitude of the spectral change, $\Delta A_{504-448}$, was plotted as a function of added $NADP^+$ (Figure 2B), and the experimental curve was fitted to eq 1 for a single binding site and unknown maximal amplitude:

$$A = A_{max}/2([E]_t + [L]_t + K_d - \sqrt{([E]_t + [L]_t + K_d)^2 - 4[E]_t[L]_t}) \quad (1)$$

where A and A_{max} are observed and maximal spectral changes, $[E]_t$ and $[L]_t$ are the total concentrations of the enzyme and ligand, respectively, and K_d is the dissociation constant. The best fit to the above equation gave a K_d value of 11.8 ± 2.6 μM and ΔA_{max} of 1.8 ± 0.1 AU/mM. Thus, the K_d of BMR for $NADP^+$ measured spectrophotometrically is about 20 times larger than that obtained by the same procedure for intact P450BM3 (see ref *15* and above). Because of this discrepancy and because of the significance of the enzyme affinity for $NADP^+$ to our understanding of the mechanism of electron transfer, we felt that it was important to reassess the affinity of intact P450BM3 for $NADP^+$ by additional and independent procedures.

Binding of [^{32}P]NADP by P450BM3. The attempt to measure [^{32}P]$NADP^+$ binding by equilibrium dialysis was unsuccessful because of the enzyme inactivation during long incubations. We therefore developed a direct and rapid assay to measure binding of [^{32}P]$NADP^+$ (*14*). A Scatchard plot, as shown in Figure 3A, revealed a single nucleotide binding site with a K_d of 10.2 ± 4.8 μM. The affinity of P450BM3 for $NADP^+$ is close to that obtained for BMR but differs considerably from the values obtained spectrophotometrically for intact P450BM3.

Competitive Inhibition by $NADP^+$. Another approach to measure the affinity of P450BM3 to $NADP^+$ is to measure the inhibition constant. However, the low K_m for NADPH [$K_m \sim 1$ μM (*12*)] and the need to avoid a regenerating system precluded the use of conventional techniques. We therefore developed a different procedure to study the inhibitory effect of $NADP^+$ on palmitate hydroxylation. NADPH is fluorescent with a maximum emission at 455 nm ($\lambda_{ex} = 340$ nm). Because palmitate hydroxylation is tightly coupled to NADPH consumption (*20*, *21*), the reaction can be measured by the decrease of NADPH fluorescence. To validate this approach, we measured the initial rates of palmitate hydroxylation in the presence of variable NADPH and 25 μM palmitate. The values of K_m and V_{max} obtained were 1.5 μM and 56 s^{-1}, in excellent agreement with the values obtained under steady-state conditions in the presence of an NADPH-regenerating system (*12*). We used this procedure to characterize the inhibition of palmitate hydroxylation by $NADP^+$. The initial rates of palmitate hydroxylation in the presence of different concentrations of NADPH and $NADP^+$ have been measured. The results demonstrated that $NADP^+$ was a competitive inhibitor with respect to NADPH (data not shown), and the Dixon plot gave a K_i value of 6.6 ± 3.1 μM (Figure 3B).

Affinity for $NADP^+$. When heme interference was eliminated, the affinity of the enzyme to $NADP^+$ was thus found to be relatively low (i) spectrophotometrically, using the

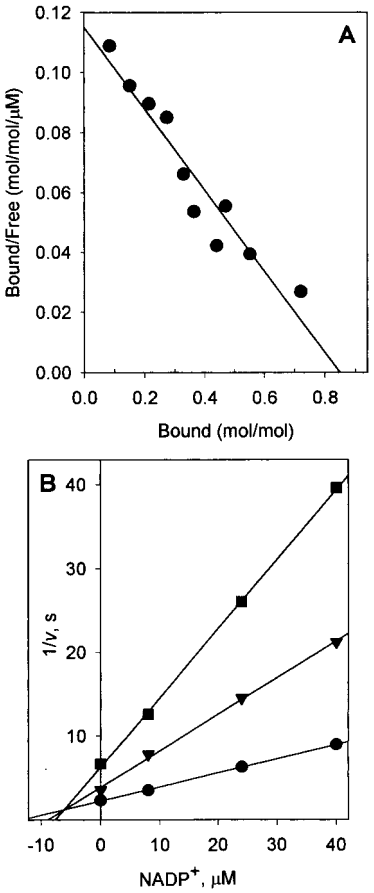

FIGURE 3: Determination of the affinity of intact P450BM3 for $NADP^+$. (A) Scatchard plot of [^{32}P]NADP binding to P450BM3. Binding was measured in the presence of 2.0 μM P450BM3 and 1−28 μM $NADP^+$. The line is a linear regression through the points. From this graph, K_d for $NADP^+$ is 7.4 μM ($r^2 = 0.92$). (B) Dixon plot of the inhibition of palmitate hydroxylation by $NADP^+$. The reaction was measured fluorometrically in the presence of 0.4 (■), 1.0 (▼), and 3.0 (●) μM NADPH. The lines are a linear regression through the data points ($r^2 \geq 0.96$). From this graph, K_i determined as the line intersection is 6.3 μM.

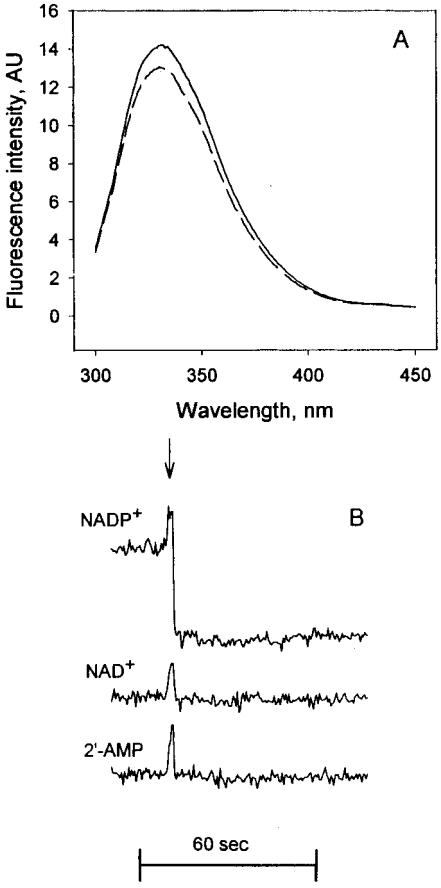

FIGURE 4: P450BM3 tryptophan fluorescence quenching by $NADP^+$ binding. (A) Fluorescence emission spectra of 0.6 μM P450BM3 in the absence (1) and presence (2) of 44 μM $NADP^+$. (B) Nucleotide specificity of the tryptophan fluorescence quenching. The arrow indicates the moment of the nucleotide additions as follows: 50 μM $NADP^+$, 50 μM NAD^+, and 100 μM 2′-AMP. Fluorescence intensity was measured with λ_{ex} 295 nm and λ_{em} 334 nm.

separated flavoprotein domain, $K_d = 11.6$ μM (Figure 2), (ii) by direct measurements of [^{32}P]$NADP^+$ binding by intact P450BM3, $K_d = 10.2$ μM (Figure 3), or (iii) by measuring the competitive inhibition constant in palmitate hydroxylation by P450BM3, $K_i = 6.6$ μM. Importantly, [^{32}P]$NADP^+$ binding represents nucleotide binding with the bulk of the P450BM3 protein, while measurements of the inhibition constant reflect nucleotide interaction with the bulk of the active enzyme catalyzing fatty acid hydroxylation. Therefore, we conclude that oxidized P450BM3 has a single binding site for $NADP^+$ with a K_d of about 10 μM.

In contrast, difference spectroscopy with intact P450BM3 produced a K_d for $NADP^+$ of 0.58 μM (*15*). We obtained a K_d of 0.7 μM using the same approach. The spectral changes in our experiments were type I binding spectra characteristic for the heme domain. The amplitude of the $NADP^+$-induced spectral change in intact P450BM3 is about 10−15% of that observed at saturating palmitate but is significantly larger than the amplitude of the spectral changes of the flavin cofactors. Importantly, no high-affinity binding was revealed by [^{32}P]$NADP^+$ binding assay or competitive inhibition studies (Figure 3). The reasons for such a binding spectrum remain unclear, but several explanations can be offered. For instance, a small fraction of the enzyme could bind nucleotide in an unusual way due to some heterogeneity of the P450BM3 preparation. Alternatively, the nicotinamide moiety could directly interact with the heme domain.

Tryptophan Fluorescence of P450BM3 and Effect of $NADP^+$. The crystal structure of rat liver P450 reductase (*22*), homologous to the reductase domain of P450BM3, demonstrated that W677 occupies the putative nicotinamide binding site. P450BM3 has 12 Trp residues, one of which, W1047, is homologous to W677 of the rat P450 reductase, and therefore nucleotide binding can be expected to change Trp fluorescence intensity. Indeed, the addition of $NADP^+$ quenched the fluorescence (Figure 4A), suggesting that the environment of some Trp residues becomes more hydrophobic upon $NADP^+$ binding, likely as a result of conformational changes. This concept has recently been confirmed using homologous ferredoxin reductase (*23*). Replacement of a bulky Tyr which occupies the nicotinamide binding site in that enzyme with a smaller residue resulted in catalytically competent nicotinamide binding.

The effect of different nucleotides on Trp fluorescence is shown in Figure 4B. Neither 50 μM NAD^+ nor 100 μM 2′-AMP significantly decreased fluorescence intensity, in contrast to the quenching observed in the presence of 50 μM $NADP^+$. Because $NADP^+$ and NAD^+ have essentially

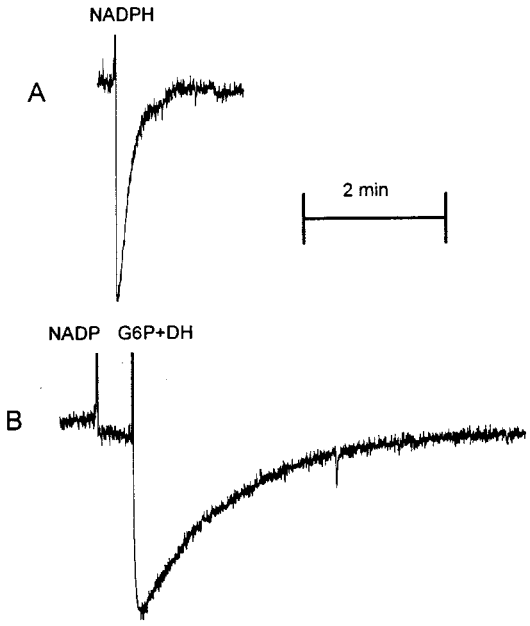

FIGURE 5: Time course of tryptophan fluorescence change upon P450BM3 interaction with NADP(H). (A) P450BM3 (0.96 μM) was mixed with 1 μM NADPH. (B) P450BM3 (0.96 μM) was mixed with 1.0 μM $NADP^+$ and 2 mM glucose 6-phosphate. G6P-DH was added to a final concentration of 0.5 unit/mL. Fluorescence intensity was measured with λ_{ex} 295 nm and λ_{em} 334 nm.

identical absorbance spectra, the fluorescence quenching in the presence of $NADP^+$ is not due to the inner filter effect but rather reflects a specific interaction of the nucleotide with the enzyme.

Interaction of P450BM3 with NADPH and $NADP^+$. Several reports with flavoproteins homologous to P450BM3 indicate that the catalytic cycle involves a change in nucleotide affinity as the state of reduction of the flavin cofactor changes (*14*, *17*, *24*, *25*). Moreover, our measurements at [P450BM3] > [NADPH] gave a K_m for NADPH of 0.3 μM (*12*), while $NADP^+$ binds with a K_d of about 10 μM (see above). To gain a better understanding of the catalytic mechanism of P450BM3, the possible alteration in nucleotide affinity was assessed using nucleotide-induced Trp fluorescence quenching.

Addition of 1.0 μM NADPH to a 0.96 μM P450BM3 solution resulted in a rapid decrease of the Trp fluorescence intensity, followed by a slower increase to the original level (Figure 5A). Measurements of the rate constant of fluorescence recovery produced a value of 0.13 ± 0.02 s^{-1}, close to the rate of oxidation of the active 2-electron reduced enzyme of 0.2 s^{-1} measured earlier (*12*). Thus, the fluorescence decrease corresponds to the binding of NADPH, and $NADP^+$ formed remains bound to the 2-electron reduced enzyme. As the flavoprotein is oxidized by oxygen, $NADP^+$ is released due to its low affinity.

In another experiment, shown in Figure 5B, 1 μM $NADP^+$ was added to a fluorometer cell containing 0.96 μM P450BM3 and glucose 6-phosphate. This resulted in very small quenching of the Trp fluorescence intensity, as expected from the K_d of about 10 μM (see above). Upon addition of G6P-DH, a rapid decrease of the fluorescence intensity was observed, followed by a slow increase to the original fluorescence level. The rate constant of fluorescence

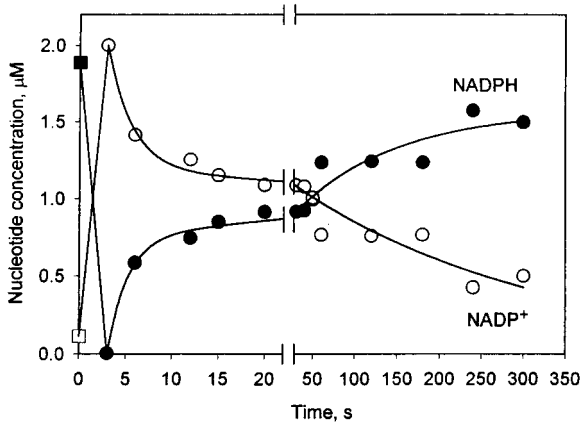

FIGURE 6: [^{32}P]NADP(H) composition changes during incubation with P450BM3. P450BM3 and NADPH concentrations were 2 μM. Square symbols represent the nucleotide composition before P450-BM3 addition.

recovery in Figure 5B of 0.013 ± 03 s^{-1} is close to the rate constant of formation of the catalytically inactive 3-electron reduced enzyme of 0.01 s^{-1} (*12*, *16*). We interpret this result to show that oxidized P450BM3 did not bind $NADP^+$ but bound NADPH rapidly formed after the addition of the G6P-DH, resulting in Trp fluorescence quenching. A prolonged incubation with NADPH led to the formation of the inactive 3-electron reduced enzyme which no longer bound NADPH with high affinity, and Trp fluorescence returned to its original level. Importantly, fluorescence quenching upon $NADP^+$ reduction is not caused by the light absorbance by the NADPH formed. Indeed, after a 5 min incubation almost all of the nucleotide is present as NADPH (see below), but tryptophan fluorescence is not quenched.

Studies with [^{32}P]NADP(H). An experiment was designed to evaluate changes of the NADP(H) reduction state under the experimental conditions of Figure 5. The enzyme was incubated with [^{32}P]NADPH and the regenerating system, and at the time indicated aliquots were withdrawn for determination of the nucleotide composition (Figure 6). In the absence of P450BM3, G6P-DH completely reduced 2 μM $NADP^+$ within a mixing time of less than 3 s (data not shown). When P450BM3 is mixed with [^{32}P]NADPH, a rapid oxidation of the nucleotide occurs. In the first 10−15 s after P450BM3 addition most of the radioactivity is found as $NADP^+$, demonstrating that most of the [^{32}P]nucleotide is bound to P450BM3 and is not readily accessible to G6P-DH. As the reaction proceeds and inactive 3-electron reduced enzyme is formed, most of the ^{32}P-labeled nucleotide is converted to NADPH. The incomplete reduction of the radiolabeled nucleotide (Figure 6) reflects an incomplete inactivation of the enzyme, which retains 20−25% of the activity (*2*, *16*) and is expected to bind $NADP^+$.

The results of Figure 6 demonstrate that our interpretation of the tryptophan fluorescence results (Figure 5) is correct: fluorescence quenching reflects binding of NADP(H). The results of Figures 5 and 6 lead to two important conclusions. (1) The nucleotide binding site is saturated in the presence of 1−2 μM P450BM3 and stoichiometric NADPH, demonstrating that the K_d of the active 2-electron reduced P450BM3 to $NADP^+$ is well below 1 μM. (2) The 3-electron reduced inactive P450BM3 is no longer able to bind reduced nucleotide with high affinity.

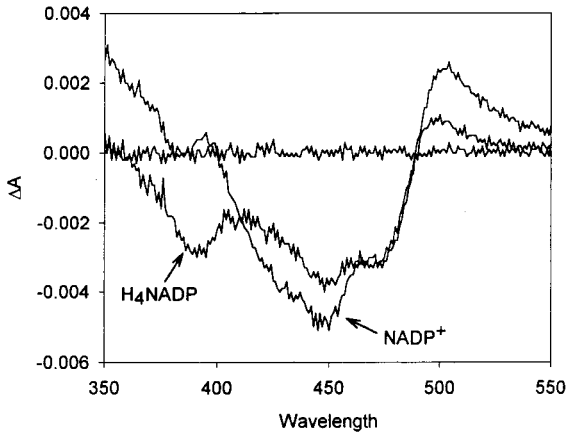

FIGURE 7: Comparison of the spectral changes associated with H_4-NADP and $NADP^+$ binding with BMR. Difference spectra were obtained in the presence of 100 μM nucleotide and 4.6 μM BMR.

Interaction with H_4-NADP. We used 1,4,5,6-tetrahydro-NADP (H_4-NADP), an analogue of the reduced nucleotide, to estimate the affinity of P450BM3 for NADPH. The structure and properties of this nucleotide, a close isosteric analogue of NADPH, are described elsewhere (*14* and references cited therein). The analogue served as a competitive inhibitor with respect to NADPH, with a K_i value of 4.5 ± 0.3 μM in the palmitate hydroxylation reaction (data not shown).

The interaction with H_4-NADP was further studied by difference spectroscopy. The analogue induced spectral changes of intact P450BM3 (data not shown) similar to those observed with $NADP^+$ (Figure 1A). The amplitude of the decrease of the heme absorbance at 420 nm exceeded manyfold the amplitude of the flavin absorbance change. This precluded any meaningful measurements with intact P450BM3, and BMR was used for further studies. H_4-NADP caused spectral changes in the flavin absorbance region (Figure 7). A plot of the amplitude $\Delta A_{499-448}$ on the analogue concentration produced a binding curve similar to that shown in Figure 2B, and best fit to eq 1 produced a K_d of 21.0 ± 4.8 μM and a maximum amplitude of 1.2 ± 0.1 AU/mM.

Interestingly, $NADP^+$ and H_4-NADP induce different spectral changes upon binding to BMR (Figure 7). This suggests a differential binding of the positively charged oxidized and of the neutral reduced nicotinamide moieties with the oxidized flavoprotein. This is in accord with our recent studies on eukaryotic P450 reductase, where reduced but not oxidized nicotinamide interacts with the flavoprotein (*14*).

Spectroscopic measurements of H_4-NADP binding with BMR produced a K_d of 21 μM, while inhibition constant measurements produced a value of 4.5 μM. The two assays differ significantly: BMR at 4.6 μM has been used in spectroscopic studies, while K_i measurements were carried out in the presence of nanomolar concentrations of intact P450BM3. It is unclear whether the difference in the measured values reflects differences in the properties of the nucleotide binding sites of BMR and P450BM3 or a 1000-fold difference in protein concentration in the assays. It is clear, however, that the K_d for H_4-NADP is at least 1 order of magnitude greater than the K_m for NADPH measured at [P450BM3] > [NADPH] (*12*). Because H_4-NADP served as a close isosteric analogue of NADPH with P450 reductase (*14*), we conclude that the affinity of NADPH to the enzyme is close to that of H_4-NADP, that is, a K_d of about 10 μM.

Asymmetry of Nucleotide Binding. A low affinity of the oxidized P450BM3 for $NADP^+$ follows from the measurements of nucleotide binding as well as from the lack of tryptophan fluorescence quenching in the presence of 1 μM P450BM3 and stoichiometric nucleotide (Figure 5B). In contrast, in the presence of 1 μM each P450BM3 and NADPH, all of the nucleotide is bound to the oxidized enzyme, and $NADP^+$ formed after hydride ion transfer is retained by the active 2-electron reduced enzyme (Figure 6). Therefore, the affinity of the 2-electron reduced P450BM3 for $NADP^+$ must be at least an order of magnitude higher than that of the oxidized enzyme. This affinity change must be associated with hydride ion transfer as H_4-NADP, a redox inactive analogue, failed to bind with high affinity.

The increased affinity of the active 1- and/or 2-electron reduced enzyme for $NADP^+$ can serve as a mechanism to prevent binding of another NADPH and formation of the inactive 3-electron reduced enzyme. The inactive enzyme has low affinity for NADPH, and no binding can be detected. The inability to bind NADP(H) could be the reason the 3-electron reduced flavoprotein cannot rapidly reduce the heme iron (*16*), as interaction of the bound NADP(H) with P450BM3 is essential for high catalysis rate (*12*). Moreover, this mechanism supports the concept of the 0-2-1-0 catalytic cycle of the flavoprotein domain of P450BM3 (*12*).

NADPH Analogues as Electron Donors. The use of the nucleotide analogues enabled us to characterize electron transfer steps in microsomal P450 reductase (*14*). The NADP(H) analogues AcPy-NADP(H) and S-NADP(H) were used to evaluate further the interaction of P450BM3 with nucleotides and to characterize the electron transfer steps. These analogues undergo the same redox transition as NADP(H), i.e., hydride ion transfer (*26*). However, the redox potentials of the analogues are quite different from that of NADPH (*26*−*28*).

The reduced analogues served as electron donors in the palmitate hydroxylation reaction (Table 1). Even though both analogues supported relatively fast catalytic turnover, both K_m and V_{max} values with AcPy-NADPH are significantly different from those of NADPH. Maximal velocities with the analogues are close to those observed with NADH, despite the fact that the K_m values differ by 2−3 orders of magnitude. A comparison of the nucleotide redox potentials and reaction rates reveals that the 73 mV difference between NADPH and AcPy-NADPH has little, if any, effect on the catalysis rate. According to the Nernst equation, a 29 mV difference in a 2-electron transfer reaction corresponds to a 1 order of magnitude change in the equilibrium constant. Thus the equilibrium of the hydride ion transfer step with AcPy-NADPH is shifted toward the reduced analogue by a factor of 330 compared to the equilibrium with NADPH. In contrast, even though redox potentials are the same, the catalysis rates with NADH are only about 20% of those with NADPH. The results of Table 1 thus demonstrate the lack of any correlation between nucleotide redox potential and catalysis rate.

Transhydrogenase Reaction and Reversibility of Hydride Ion Transfer. To assess the possible reversal of the hydride ion transfer step between NADPH and FAD, we measured

Table 1: Kinetic Parameters of 250 μM Palmitate Hydroxylation and 50 μM Cytochrome *c* Reduction in the Presence of NADPH and the Analogues[a]

		palmitate hydroxylation		cytochrome *c* reduction	
nucleotide	E_0, mV[b]	V_{max}, s^{-1}	K_m, μM	V_{max}, s^{-1}	K_m, μM
NADH[c]	−320	13 ± 1	3960 ± 457	22 ± 5	2691 ± 907
NADPH	−320	68 ± 5	1.4 ± 0.1	102 ± 17	1.2 ± 0.1
S-NADPH	−285	25.3 ± 3.5	2.0 ± 0.7	65.4 ± 7.9	0.71 ± 0.15
AcPy-NADPH	−247	13.2 ± 4.1	11.1 ± 4.6	14.5 ± 2.0	11.5 ± 2.4

[a] Average ± SD of at least three measurements is shown. [b] Redox potentials are from refs *27* and *28*. [c] Results with NADH are from ref *12*.

Table 2: Transhydrogenase Activities Catalyzed by P450BM3 and Mutant Proteins[a]

donor	acceptor	P450BM3	BMR	W574Y	W574G	G570D
NADPH	AcPy-$NADP^+$	7.1 ± 0.3	9.8 ± 0.4	7.8 ± 0.2	37.3 ± 1.6	21.0 ± 1.3
NADPH	S-$NADP^+$	15.0 ± 0.8	18.0 ± 2.4	13.6 ± 0.4	55.3 ± 3.1	33.7 ± 1.8
NADPH	[^{3}H]$NADP^+$	8.3 ± 1.6	8.0 ± 2.2	8.6 ± 1.7	23.8 ± 2.1	13.4 ± 0.7
S-NADPH	$NADP^+$	3.3 ± 0.2	4.1 ± 0.2	3.4 ± 0.1	11.5 ± 1.1	6.6 ± 0.6
AcPy-NADPH	$NADP^+$	0.63 ± 0.04	0.55 ± 0.03	0.70 ± 0.07	1.71 ± 0.05	1.13 ± 0.17

[a] Rates shown are in s^{-1}. Average ± SD of four measurements is shown.

the transhydrogenase reaction between NADPH and oxidized nucleotides (Table 2). No detectable transhydrogenase reaction occurred in the absence of P450BM3. In the presence of P450BM3, a rapid transhydrogenation occurred with rates of 7, 15, and 8 s^{-1} with AcPy-$NADP^+$, S-$NADP^+$, and $NADP^+$ as electron acceptors, respectively. The reduced analogues also serve as donors in the transhydrogenase reaction with $NADP^+$ as acceptor (Table 2). Although relatively slow, P450BM3 catalyzes hydride transfer from AcPy-NADPH to $NADP^+$, against a 73 mV redox potential difference.

Transhydrogenase rates are much faster than the rate of 2-electron reduced enzyme oxidation and formation of the inactive 3-electron reduced P450BM3 [0.2 s^{-1} and 0.01 s^{-1}, respectively (*12*)]. Thus the transhydrogenase reaction involves reduction of $NADP^+$ or its analogue by the active, 2-electron reduced P450BM3. As the rate of electron transfer to FMN is at least 400 s^{-1} (*16*), a significant fraction of the 2-electron reduced enzyme is present as a double semiquinone form (*12*). Therefore, the transhydrogenase reaction must include the reverse reaction, fast electron transfer from FMN semiquinone to FAD semiquinone.

Table 2 also shows transhydrogenase activities of BMR and three FMN binding site mutants, W574Y, W574G, and G570D (*29*). BMR and W574Y, carrying both FAD and FMN, catalyzed the reaction with rates close to those of the wild-type enzyme. In contrast, the catalysis rates of the FMN-free mutants, W574G and G570D, were severalfold higher than the rates of wild-type P450BM3. The higher reaction rates observed with FMN-free mutants are explained by the fact that the lack of electron transfer to FMN increases the steady-state fraction of FAD hydroquinone, which serves as the hydride ion donor for the bound $NADP^+$. These results demonstrate that the transhydrogenase reaction involves only the FAD cofactor and hydride ion transfer between NADPH and FAD is readily reversible.

The mechanism of transhydrogenase reaction is the same as we defined for P450 reductase (*14*) and can be outlined as follows. P450BM3 binds NADPH and accepts 2 electrons, and the $NADP^+$ formed is released. An $NADP^+$, or its analogue, will bind to the 2-electron reduced protein, and the electron-transfer reactions described above will reverse to transfer hydride ion to the bound analogue, which is released into the medium.

The transhydrogenase reaction demonstrates that both bound $NADP^+$ and NADPH are able to dissociate within a fraction of a second. On the other hand, the results of Figures 5 and 6 demonstrate that nucleotide remains bound for seconds or even minutes. This tight binding is a result of a rapid dynamic equilibrium when bound nucleotide has high *on* and *off* rates, but the thermodynamic equilibrium is shifted toward complex formation due to the high affinity. This, in turn, indicates that the affinity of the enzyme to the nucleotide after hydride ion transfer is considerably higher than that before the enzyme reduction. This is consistent with our notion that hydride ion transfer is accompanied by at least a 10-fold change in the enzyme affinity to $NADP^+$, which would correspond to a $\geq$30 mV shift in redox potential of the bound nicotinamide and/or flavin nucleotides.

Redox Potentials of the Flavin Cofactors during Catalysis. The equilibrium redox potentials of the P450BM3 flavin cofactors have been determined (*11*). These values are inconsistent with the enzyme's behavior during catalysis. (1) A double semiquinone form of the enzyme is clearly present during catalysis (*12*) yet should not be formed. (2) An inactive FMN hydroquinone form of P450BM3 should form within milliseconds, in contrast to the measured rate of inactivation of about 0.01 s^{-1} (*16*).

Assuming that the NADPH concentration is saturating, we calculated the equilibrium constants and some of the rate constants to characterize the interaction of NADPH with the enzyme and to define catalytic intermediates (Figure 8). However, it should be noted that equilibrium constants will not change at lower NADPH concentration, because these reactions are monomolecular. Our approach is defined as follows.

EPR measurements of the semiquinone content produced a value of 1.22 mol/mol of enzyme (*12*). Half of this value, 0.61, represents the fraction of the 2-electron reduced enzyme present as a double semiquinone form (complex 3). The rate of $FADH_2$ oxidation of the W574G mutant enzyme of 0.035 s^{-1} (*12*) is much slower than the rate of the NADPH−[^{3}H]$NADP^+$ transhydrogenase reaction of 23.8 s^{-1} (Table 2). Thus, during catalysis, the mutant enzyme is present as

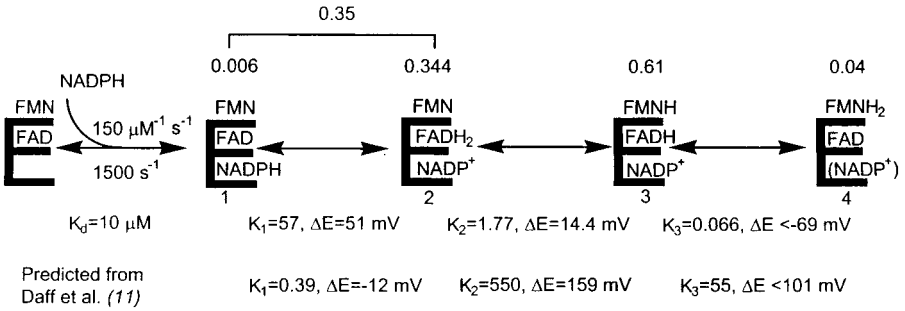

FIGURE 8: Distribution of P450BM3 flavoprotein domain species during catalysis calculated on the basis of the experimental results. Enzyme complexes emerging after NADPH binding are numbered 1−4. The numbers above the complexes represent the fraction of the enzyme present as the complex. $NADP^+$ in complex 4 is in parentheses because no evidence is available as to whether this complex retains bound nucleotide. Also shown are the values calculated from the equilibrium redox potentials measured elsewhere (*11*). See text for details.

either the FAD−NADPH or $FADH_2$−$NADP^+$ form (complexes 1 and 2, respectively). Hence, the ratio of the transhydrogenation rate of the wild-type P450BM3 to that of the W574G mutant enzyme, 8.3/23.8 = 0.35, represents the fraction of the wild-type P450BM3 with fully oxidized FMN. Thus, the fraction of the protein with fully reduced FMN equals 0.04.

Using a k_{on} for NADPH of 15×10^7 M^{-1} s^{-1} (*12*) and an estimated K_d of 10 μM (see above), one can calculate the rate of NADPH release, $k_{off} = K_d k_{on}$, as 1500 s^{-1}. As the rate of the NADPH−[^{3}H]$NADP^+$ transhydrogenase reaction by the W574G mutant is 23.8 s^{-1}, the fraction of the enzyme present as complex 1 can be calculated as a ratio $23.8/k_{off}$ = 0.006, and the fraction of the enzyme present as complex 2 is 0.344. The fractional distribution of the enzyme between complexes 1−4 allows us to calculate the equilibrium constants for each step, $K_1 = 57$, $K_2 = 1.77$, $K_3 = 0.066$, and these equilibrium constants can be converted to the redox potential changes using the Nernst equation. It should be emphasized that these are the values for the conversion of one complex to another, not the transitions of individual cofactor(s). The values expected from the equilibrium redox potentials (*11*) are also presented in the scheme. Remarkably, the equilibrium constants operating during catalysis and those measured under thermodynamic equilibrium in the absence of NADP(H) bound differ by at least 2 orders of magnitude. Thus, the role of the bound nucleotide in P450BM3 catalysis is to tailor and maintain redox potentials of the flavin cofactors so that rapid catalysis can occur. This can be achieved by direct interaction of the redox cofactors (*30*) or by conformational changes leading to an alteration of the environment of the isoalloxazine rings. For instance, single amino acid substitutions or modification of the surface charge distribution in flavodoxin, myoglobin, or cytochrome b_5 can result in as large as 100−200 mV shifts of redox potentials (*31*−*33*).

The scheme of Figure 8 allows us to predict the shift in the apparent enzyme affinity for NADP(H) associated with hydride ion transfer. Indeed, K_d is defined as $[E_{free}]$-$[NADPH_{free}]$/[complex 1], while K_m is defined as $[E_{free}]$-$[NADPH_{free}]/\sum$[complexes 1−4]. Thus K_m must be less than K_d, which is in agreement with our earlier studies (*12*).

The relevance of the complexes to P450BM3 catalysis deserves mention. The rate of hydride ion transfer by P450BM3 has been measured as 760−770 s^{-1} (*34*), while the rate of electron transfer from the FAD hydroquinone to the oxidized FMN is at least 400 s^{-1} as measured by the rate of cytochrome *c* reduction (*16*). The rates of FMN to heme electron transfer of 220−250 s^{-1} (*34*, *35*) is still slower than the minimal estimate for intramolecular electron transfer. Therefore, the enzyme complexes shown in Figure 8 should form before electron transfer to the heme iron occurs, and FMN semiquinone of complex 3 will serve as the electron donor for the heme iron and is an intermediate of fatty acid hydroxylation. The sequence of the second electron transfer to the heme and $NADP^+$ release remains to be determined. However, we have already demonstrated that binding of a single molecule of NADPH is sufficient to complete the full catalytic cycle (*12*).

A comparison of the properties of P450BM3 to those of house fly P450 reductase (*14*) shows significant differences in the properties of the two enzymes. Intramolecular hydride ion transfer in P450 reductase occurs with little free energy change, while the equilibrium is significantly shifted toward $FADH_2$ in P450BM3. A majority of the enzyme is present as a double semiquinone form in P450BM3, compared to only one-fifth in P450 reductase. Oxidized P450 reductase has a much higher affinity to NADPH, but no significant change in affinity is associated with hydride ion transfer. In contrast, the affinity of P450BM3 for NADPH is relatively low, but a significant increase in the affinity occurs upon hydride ion transfer, and the oxidized nucleotide remains bound. This mechanism could have evolved as a protection against oxidation of intracellular NADPH and inactivation of P450BM3.

ACKNOWLEDGMENT

We thank Professor Armand Fulco for the generous gift of the expression plasmids for the wild type and FMN-free mutant P450BM3 and Dr. Andrew Munro for the generous gift of the BMR expression vector.

REFERENCES

1. Porter, T. D. (1991) *Trends Biochem. Sci. 16*, 154−158.
2. Narhi, L. O., and Fulco, A. J. (1986) *J. Biol. Chem. 261*, 7160−7169.
3. Wen, L.-P., and Fulco, A. J. (1987) *J. Biol. Chem. 262*, 6676−6682.
4. Narhi, L. O., and Fulco, A. J. (1987) *J. Biol. Chem. 262*, 6683−6690.
5. Nakayama, N., Takemae, A., and Shoun, H. (1996) *J. Biochem. 119*, 435−440.
6. Griffith, O. W., and Stuehr, D. J. (1995) *Annu. Rev. Physiol. 57*, 707−736.
7. Marletta, M. A. (1993) *J. Biol. Chem. 268*, 12231−12234.

8. Vermilion, J. L., and Coon, M. J. (1978) *J. Biol. Chem. 253*, 8812−8819.
9. Vermilion, J. L., Ballou, D. P., Massey, V., and Coon, M. J. (1981) *J. Biol. Chem. 256*, 266−277.
10. Klein, M. L., and Fulco, A. J. (1993) *J. Biol. Chem. 268*, 7553−7561.
11. Daff, S. N., Chapman, S. K., Turner, K. L., Holt, R. A., Govindaraj, S., Poulos, T. L., and Munro, A. W. (1997) *Biochemistry 36*, 13816−13823.
12. Murataliev, M. B., Klein, M., Fulco, A., and Feyereisen, R. (1997) *Biochemistry 36*, 8401−8412.
13. Murataliev, M. B., Ariño, A., Guzov, V. M., and Feyereisen, R. (1999) *Insect Biochem. Mol. Biol. 29*, 233−242.
14. Murataliev, M. B., and Feyereisen, R. (2000) *Biochemistry 39*, 5066−5074.
15. Black, S. D., Linger, M. H., Freck, L. C., Kazemi, S., and Galbraith, J. A. (1994) *Arch. Biochem. Biophys. 310*, 126−133.
16. Murataliev, M. B., and Feyereisen, R. (1996) *Biochemistry 35*, 15029−15037.
17. Murataliev, M. B., and Feyereisen, R. (1999) *FEBS Lett. 453*, 201−204.
18. Lowry, O. H., Rosebrough, N. J., Farr, A. L., and Randall, R. J. (1951) *J. Biol. Chem. 195*, 265−275.
19. Segel, I. H. (1975) *Enzyme Kinetics*, p 73, Wiley-Interscience, New York.
20. Matson, R. S., Hare, R. S., and Fulco, A. J. (1977) *Biochim. Biophys. Acta 487*, 487−494.
21. Boddupalli, S. S., Estabrook, R. W., and Peterson, J. A. (1990) *J. Biol. Chem. 265*, 4233−4239.
22. Wang, M., Roberts, D. L., Paschke, R., Shea, T. M., Masters, B. S., and Kim, J. J. (1997) *Proc. Natl. Acad. Sci. U.S.A. 94*, 8411−8416.
23. Deng, Z., Aliverti, A., Zanetti, G., Arakaki, A. K., Ottado, J., Orellano, E. G., Calcaterra, N. B., Ceccarelli, E. A., Carrillo, N., and Karplus, P. A. (1999) *Nat. Struct. Biol. 6*, 847−853.
24. Lambeth, J. D., and Kamin, H. (1976) *J. Biol. Chem. 251*, 4299−4306.
25. Batie, C. J., and Kamin, H. (1986) *J. Biol. Chem. 261*, 11214−11223.
26. Kaplan, N. O. (1960) in *The Enzymes* (Boyer, P. D., Lardy, H., and Myrbäck, K., Eds.) Vol. 3, pp 105−169, Academic, New York.
27. Kaplan, N. O., Ciotti, M. M., and Stolzenbach, F. E. (1956) *J. Biol. Chem. 221*, 833−844.
28. Anderson, B. M., and Kaplan, N. O. (1959) *J. Biol. Chem. 234*, 1226−1232.
29. Klein, M. L., and Fulco, A. J. (1993) *J. Biol. Chem. 268*, 7553−7561.
30. Blankenhorn, G. (1975) *Eur. J. Biochem. 50*, 351−356.
31. O'Farrell, P. A., Walsh, M. A., McCarthy, A. A., Higgins, T. M., Voordouw, G., and Mayhew, S. G. (1998) *Biochemistry 37*, 8405−8416.
32. Varadarajan, R., Zewert, T. E., Gray, H. B., and Boxer, S. G. (1989) *Science 243*, 69−72.
33. Rivera, M., Wells, M. A., and Walker, F. A. (1994) *Biochemistry 33*, 2161−2170.
34. Munro, A. W., Daff, S., Coggins, J. R., Lindsay, J. G., and Chapman, S. K. (1996) *Eur. J. Biochem. 239*, 403−409.
35. Hazzard, J. T., Govindaraj, S., Poulos, T. L., and Tollin, G. (1997) *J. Biol. Chem. 272*, 7922−7926.

BI001068U